

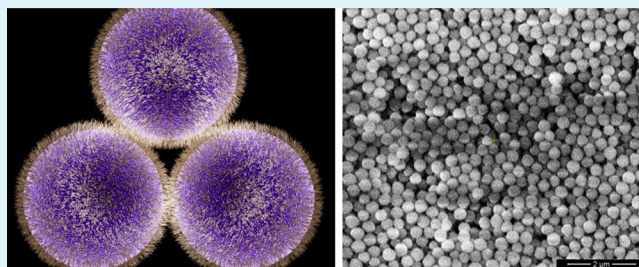
# Reversible Assembly of Tunable Nanoporous Materials from “Hairy” Silica Nanoparticles

Amir Khabibullin, Emily Fullwood, Patrick Kolbay, and Ilya Zharov\*

Department of Chemistry, University of Utah, Salt Lake City, Utah 84112, United States

**ABSTRACT:** Membranes with 1–100 nm nanopores are widely used in water purification and in biotechnology, but are prone to blockage and fouling. Reversibly assembled nanoporous membranes may be advantageous due to recyclability, cleaning, and retentate recovery, as well as the ability to tune the pore size. We report the preparation and characterization of size-selective nanoporous membranes with controlled thickness, area, and pore size via reversible assembly of polymer brush-grafted (“hairy”) silica nanoparticles. We describe membranes reversibly assembled from silica particles grafted with (1) polymer brushes carrying acidic and basic groups, and (2) polymer brushes carrying neutral groups. The former are stable in most organic solvents and easily disassemble in water, whereas the latter are water-stable and disassemble in organic solvents.

**KEYWORDS:** nanoporous, reversible assembly, polymer-grafted particles, ultrafiltration, membrane



## INTRODUCTION

Ultrafiltration (UF) is used on the industrial scale<sup>1</sup> and in research laboratories for separations of inorganic and biological nanoparticles and synthetic and biological macromolecules.<sup>2,3</sup> Nanoporous membranes are also used in biosensing,<sup>4,5</sup> drug delivery,<sup>6</sup> catalysis<sup>7,8</sup> and optics.<sup>9</sup> Many of these applications require control over the pore size, a narrow pore size distribution,<sup>10</sup> functional membrane surface, chemical and thermal stability, and simple and economical preparation processes.<sup>11</sup>

The typical materials used for nanoporous membrane preparation are polymers,<sup>12–14</sup> ceramics<sup>15,16</sup> and zeolites.<sup>17</sup> Regardless of the material, these nanoporous membranes are formed via irreversible covalent bonds and often suffer from pore blocking and surface fouling during operation. In contrast, membranes formed by noncovalent reversible assembly of molecular or nanoscale building blocks may provide a useful alternative in terms of fabrication, processing, cleaning, and reusing.<sup>18–21</sup>

Self-assembly of colloidal particles into nanoporous membranes would allow combining the advantages of reversibility with easy pore size tunability, cheap building blocks, and attractive material properties, such as flexibility. Previously, mechanically deposited colloidal particle layers have been proposed for use in industrial water treatment,<sup>22,23</sup> but they provide only crude separations. So far, only gold nanoparticles were used to form self-assembled nanoporous membranes,<sup>24–26</sup> although other inorganic nanoparticles have been assembled into superstructures.<sup>27,28</sup> Self-assembled gold nanoparticle membranes showed promising nanofiltration characteristics,<sup>26</sup> but the small size of the gold nanoparticles and their high cost limit scaling up and achieving a broader pore size range of such

membranes. Assembling silica colloidal spheres into ultrafiltration membranes would provide a cheap alternative while allowing for flexibility in the pore size.

Recently, we prepared selective and responsive self-assembled supported colloidal films,<sup>29</sup> and covalently bound free-standing colloidal membranes<sup>30</sup> using silica nanospheres. They possess size-selectivity tunable by changing the silica particle size<sup>31</sup> and are capable of charge-<sup>30</sup> and enantioselective<sup>32</sup> transport after the suitable silica surface modification. The covalently formed silica colloidal membranes are mechanically, thermally, and chemically stable, but are rigid and have to be prepared by sintering at 1050 °C.<sup>30</sup> In this work, we report the reversible formation of flexible nanoporous membranes via the self-assembly of silica nanospheres modified with polymer brushes. Membranes were prepared using silica spheres carrying acidic poly(3-sulfopropyl methacrylate), PSPM, and basic poly(*N*-dimethylaminoethyl methacrylate), PDMAEMA, brushes. The preparation process of these “acid-base membranes” involved mixing two colloidal solutions of silica spheres and drying the solvent. The second type of nanoporous membranes, “neutral membranes”, was prepared using silica spheres carrying poly(hydroxyethyl methacrylate), PHEMA, brushes and the membranes were prepared by the deposition of PHEMA-modified silica spheres from ethanol.

## MATERIALS AND METHODS

**Materials.** Copper(I) chloride (anhydrous, 99.99%), Copper(II) chloride (99.99%), 1,1,4,7,10,10-hexamethyltriethylenetetramine

**Received:** August 29, 2014

**Accepted:** September 9, 2014

**Published:** September 9, 2014



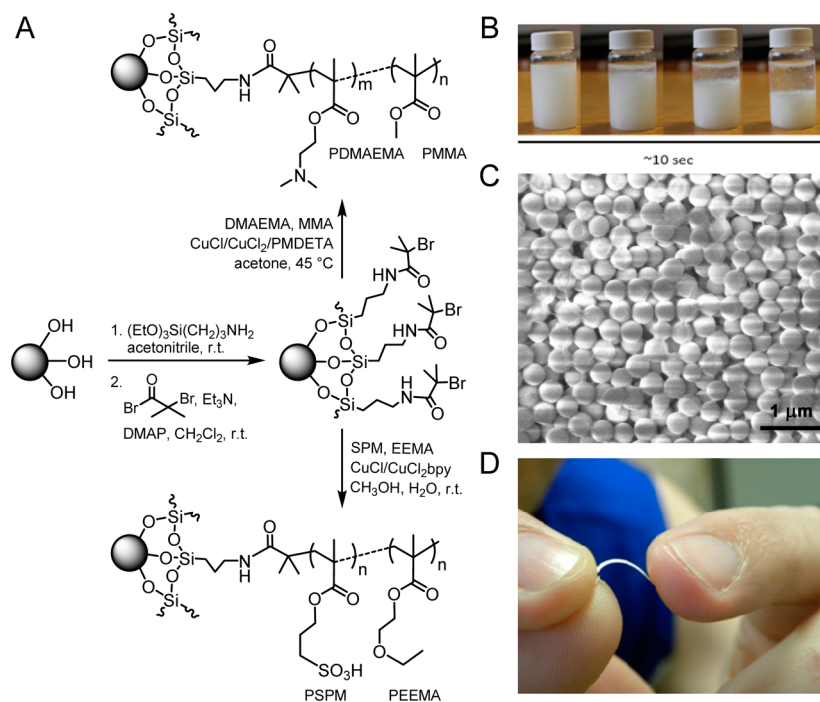


**Figure 1.** Preparation and properties of “acid–base” membranes. (A) Preparation of copolymer brushes in the surface of silica spheres. (B) Dispersion of “acid–base” membranes in ethanol and gel formation. (C) Representative SEM image of “acid–base” membrane. (D) Flexible “acid–base” membrane.

(HMTETA, 97%), tetraethyl orthosilicate (99.99%), ethyl 2-bromoisobutyrate (98%), 3-aminopropyltriethoxysilane (APTES, 98%), 2-bromoisobutyryl bromide (98%), 2,2'-dipyridyl (99%) were obtained from Aldrich and used as received. The monomers 2-(dimethylamino)ethyl methacrylate (DMAEMA, 99%), 3-sulfopropyl methacrylate (SPM, 99%), 2-ethoxyethyl methacrylate (EEMA, 98%), methyl methacrylate (MMA, 99%) and 2-hydroxyethyl methacrylate (HEMA, 98%) were obtained from Aldrich and passed through a column of basic alumina before use. Acetonitrile (Mallinckrodt, HPLC grade), triethylamine (98%, J. T. Baker), dichloromethane (Mallinckrodt, HPLC grade) were distilled from CaH<sub>2</sub> before use. Eighteen MΩ cm water was obtained from a Barnsted “E-pure” water purification system.

**Characterization.** Scanning electron microscopy (Hitachi S3000–N) was employed to perform the imaging of the materials. Thermogravimetric analysis of polymer-modified particles was conducted using TGA 2950 Thermogravimetric Analyzer (TA Instruments). Fisher Scientific Isotemp Programmable Muffle Furnace (model 650) was used for calcination. Branson 1510 sonicator was used for all sonications. UV/vis measurements were performed using an Ocean Optics USB2000 or USB4000 instrument.

**Preparation of Silica Spheres.** All silica spheres were prepared according to previously reported procedure.<sup>33</sup> The spheres were purified by several cycles of suspending in ethanol and water with sonication followed by centrifugation. The silica spheres were dried in a stream of nitrogen for 12 h and calcinated at 600 °C for 4 h. SEM images of the spheres were obtained and the diameters determined to be 390 ± 20 nm (for the particles prepared using the final concentrations of 0.2 M TEOS, 0.6 M NH<sub>4</sub>OH and 17 M H<sub>2</sub>O), 280 ± 30 nm (0.6 M TEOS, 0.6 M NH<sub>4</sub>OH, and 17 M H<sub>2</sub>O), 460 ± 50 nm (1.2 M TEOS, 0.6 M NH<sub>4</sub>OH, and 17 M H<sub>2</sub>O).

**Preparation of Polymer-Modified Silica Spheres.** The calcinated silica spheres were rehydroxylated and modified with 2-bromoisobutyryl bromide (ATRP initiator) as reported earlier.<sup>34</sup> The PSPM-r-PEEMA and PDMAEMA-r-PMMA brushes were grown on the surface of silica spheres via ATRP according to the previously reported procedures.<sup>34,35</sup> The grafting of PSPM and PSPM-r-PEEMA brushes onto the initiator-modified silica spheres (1 g) was carried out in a 2:1 (by weight) mixture of degassed methanol and water,

containing 2,2'-dipyridyl, CuCl<sub>2</sub>, CuCl, as well as equal amounts of monomers EEMA and SPM (0.01 mol of each) at room temperature for 12 h in a nitrogen atmosphere. Polymerization reaction was quenched by exposing the reaction mixture to air and addition of water. PSPM-modified silica spheres were repeatedly rinsed with water and methanol, soaked in 1 M HCl for 12 h to exchange potassium ions with protons, then the sample was rinsed with water to remove excess acid. The grafting of PDMAEMA and PDMAEMA-r-PMMA brushes onto the initiator-modified silica spheres (1 g) was carried in degassed acetone/water mixture (9:1 ratio by weight) containing 2,2'-dipyridyl, CuCl<sub>2</sub>, CuCl, as well as equal amounts of DMAEMA and MMA (0.01 mol each) at 50 °C under the nitrogen atmosphere for 12 h. The polymerization reaction was quenched by exposing the reaction mixture to air and addition of water and the particles were rinsed with ethanol. The grafting of PHEMA brushes onto the initiator-modified silica spheres (1 g) was carried out in degassed methanol containing PMDETA, CuBr<sub>2</sub>, CuBr, as well as HEMA (5.7 mmol) at 70 °C for 12 h under the nitrogen atmosphere. The resulting modified particles were washed with methanol and water.

The length of the polymer brushes prepared on the surface of the silica spheres as described above was determined using DLS and estimated using TGA.

**Assembly of Free-Standing Membranes.** The separate colloidal solutions of acidic and basic polymer-modified silica spheres (1 g each) were prepared in 10 mL of ethanol. The solutions were mixed together in a 25 mL beaker or 4 in. Petri dish and air-dried. PHEMA-modified particles were dispersed in ethanol and left to air-dry.

**Diffusion through the Membranes.** Diffusion experiments through the colloidal membranes were performed by sealing a piece of a membrane between Teflon rings and placing it between two 1 cm quartz cuvettes. The feed cell contained 4.00 mL of the permeate in ethanol or water, while the receiving cell contained 4.00 mL of ethanol or water. The flux was monitored by recording the UV–vis absorbance at 555 nm for dye-labeled dendrimers, 250 nm for PS beads, 323 nm for dansyl-labeled silica spheres, and 200 nm for Au nanoparticles in the receiving cell for at least 12 h. Prior to using a membrane in a new experiment, it was immersed in ethanol or water for at least 24 h and the solvent was replaced occasionally to ensure the removal of any previous probe molecule or particles from the membranes.

**Pressure-Driven Filtration of Nanoparticles.** A 25 mL stirred pressure filtration cell was used for these experiments. A membranes were deposited on a support by driving 10 mL of a colloidal solution under 21 psi air pressure. The support was 25 mm nylon or cellulose filter with 0.2  $\mu\text{m}$  pores. The membranes were air-dried for 15 min. Solutions containing G5 PAMAM dendrimer, 20 and 40 nm Au particles, or 25 and 39 nm PS beads were driven through the membranes by air pressure. The filtrates were analyzed using DLS and UV–vis spectroscopy. Between the runs the membranes were cleaned by driving the solvent through and air-drying for 15 min.

**Flux Measurements.** A “neutral” membrane was prepared using 460 nm silica spheres on a regenerated cellulose filter as described above. Distilled water was driven once through the cellulose filter first and then through the supported membrane (the membrane was dried for 15 min between the experiments) under the constant driving pressure of 0.35 bar (5 psi) and 1.45 bar (21 psi). Time taken to pass 4 mL of water was recorded after 1 mL of liquid had already been passed through. The flux of ethanol through the “acid–base” membrane prepared from 390 nm silica spheres modified with “acid” and “base” polymer brushes was measured following the same procedure.

**Mechanical Testing of the Membranes.** The flexural strength of the free-standing “neutral” membranes was estimated using the four-point bending test, as described elsewhere.<sup>36</sup> Rectangular membrane samples were cut using a carbon dioxide laser. The membrane sample was placed on two metal rods of the support span and covered with the loading span that made contact with the sample using two metal rods. A load was applied and increased until the membrane sample fractured, and the rupture force was used to calculate the flexural strength using the following equation:  $\sigma = (FL/bd^2)$ , where  $\sigma$  is flexural strength (Pa),  $F$  is rupture force (N),  $L$  is support length (m),  $b$  is sample width (m), and  $d$  is sample thickness (m).

## RESULTS AND DISCUSSION

**“Acid–Base” Membranes.** To form these membranes, we prepared “hairy” silica spheres using surface-initiated ATRP of 3-sulfopropyl methacrylate (SPM) and *N*-dimethylaminoethyl methacrylate (DMAEMA), as shown in Figure 1A, and varied the length of the polymer brushes using the polymerization time to find the optimal ratio of this length to the silica sphere diameter. We discovered that upon mixing two ethanol colloidal solutions containing 390 nm silica spheres modified with short PSPM and PDMAEMA brushes (10 and 40 nm, respectively, determined by thermogravimetric analysis), a gel was rapidly formed (Figure 1B) and after complete evaporation of ethanol, irregular cracked pieces of a solid material were formed. The SEM images of the “acid–base” membranes (Figure 1C) showed closely packed yet disordered silica spheres with interstitial spaces. We believe that the observed assembly of the “hairy” silica particles results from the polymer brush entanglement, responsible for holding the particles in the membrane together.<sup>25,37,38</sup>

To improve the mechanical properties of the assembled material, we added 2-ethoxyethyl methacrylate (EEMA) and methyl methacrylate (MMA) to PSPM and PDMAEMA brushes, respectively. The monomer molar ratios of 0.3:0.7 and 0.7:0.3 did not lead to better mechanical properties of the material. On the other hand, the molar ratio of 1:1 was optimal for the formation of durable, flexible, and large-area ( $\sim 1.5\text{ cm}^2$ ) crack-free membranes. We speculate that crack reduction was caused by slower solvent drying due to the higher “affinity” of neutral PMMA and PEEMA toward ethanol compared to charged PSPM and PDMAEMA, and by the reduced strength of the particle–particle interactions.<sup>39</sup>

The membranes were stable for days in organic solvents, such as ethanol, acetonitrile, acetone, DMF, and benzene. However, the membranes softened in 5–10 min and

completely dispersed within  $\sim 5$  min of sonication in water. Indeed, acidic and basic polymer brushes interact strongly in organic solvents, whereas water effectively solvates sulfonic and amino groups and disrupts these interactions, leading to weaker interactions between the polymer chains and therefore between the colloidal spheres,<sup>40</sup> resulting in membrane disassembly. Within  $\sim 10$  s after the sonication was stopped, the particles reassembled from solution into a gel (Figure 1B). The membranes reassembled after complete water evaporation and remained durable and flexible. They could withstand multiple cycles of assembly disassembly without losing their properties. SEM images confirmed that the membranes disassemble into the discrete silica spheres and that the packing of silica spheres in reassembled membranes was similar to the initially deposited membranes. Thus, the assembly of the “acid–base” materials is completely reversible.

The thickness of the assembled free-standing membranes could be controlled by the concentration of the “hairy” particles in solution. For example, it was 0.5 mm when 6 wt % concentration was used, and 1 mm for 12 wt % concentration. We found that the flexibility of the membranes depends on the thickness and the length/thickness ratio. For instance, a 10 mm long and 0.2 mm thick membranes prepared from 4 wt % solution showed significant flexibility (Figure 1D).

To demonstrate the porosity of free-standing “acid–base” membranes, we performed diffusion experiments using membranes prepared from “hairy” 390 nm silica spheres. We used Rhodamine B-labeled PAMAM dendrimer,<sup>31</sup> dansyl-labeled silica particles, and polystyrene (PS) beads in ethanol. We found that G5 PAMAM dendrimer (ca. 6 nm in diameter) diffuses quickly through these membranes, while no diffusion was observed for 100 and 250 nm dansyl-labeled silica particles. Furthermore, we found that 54 nm PS beads diffused through this membrane, while 84 nm PS beads did not diffuse. Thus, the size cutoff for this “acid–base” membrane was between 54 and 84 nm. The pore “diameter” for a close-packed colloidal crystal can be estimated as ca. 15% of the silica sphere diameter.<sup>31</sup> For the colloidal crystal made of 390 nm silica spheres this “diameter” is 59 nm, confirming that randomly packed “hairy” silica spheres produce a reasonably close-packed arrangement as well.

Next, we pressure-deposited a mixture of 390 nm silica spheres modified with PSPM/PEEMA and PDMAEMA/PMMA brushes on top of a regenerated cellulose filter with 0.2  $\mu\text{m}$  pores. The thickness of the deposited membranes could be varied from a few micrometers to ca. 0.5 mm by changing the concentration of the silica spheres in the colloidal solution. The assembly disassembly behavior of the supported “acid–base” membranes remained the same as that of the free-standing “acid–base” membranes: they could be completely dispersed in water and deposited on the same or new support.

We measured the flux of ethanol through a 0.5 mm-thick membrane under the pressure of 1.45 bar (21 psi). The average ethanol flux through the regenerated cellulose filter under this pressure was  $7600\text{ L m}^{-2}\text{ h}^{-1}$  (33 gpm), whereas that through the “acid–base” membrane under the same pressure was  $380\text{ L m}^{-2}\text{ h}^{-1}$  (1.6 gpm). This flux is comparable or exceeds the flux of commercially available ultrafiltration membranes (such as 1 gpm for Neo-Pure TL3 Ultrafiltration membrane with 25 nm filtration cutoff).

We used ethanol solutions of G5 PAMAM dendrimer and polystyrene nanoparticles to determine the filtration cutoff of the supported membrane. The 6 nm dendrimer molecules



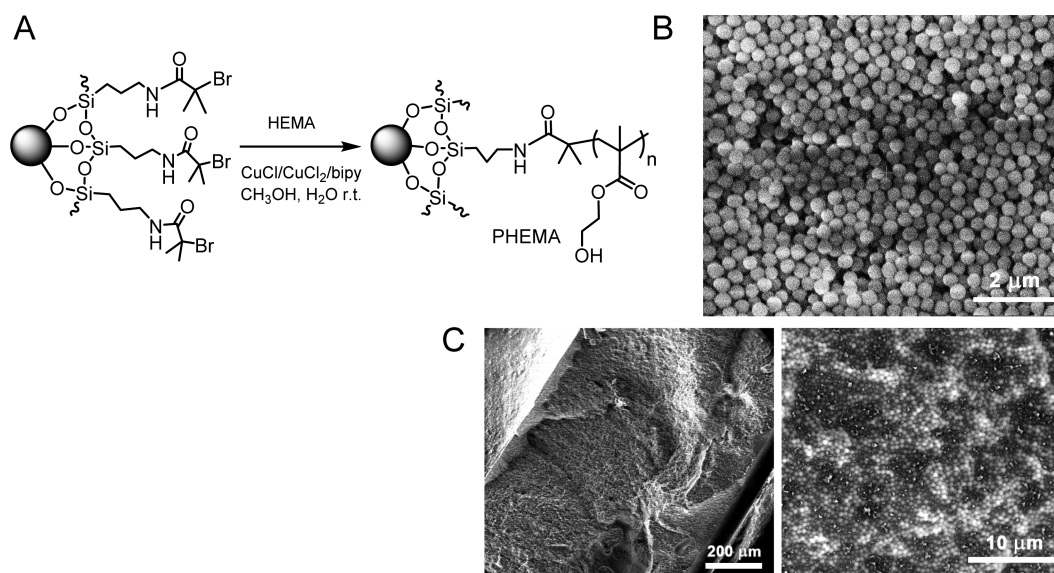


**Figure 2.** “Neutral” membrane. (A) Preparation of PHEMA brushes on the surface of silica spheres. Representative SEM images of the (B) top and (C) cross-section view of “neutral” membrane.

passed through the membrane, while 39 nm polystyrene beads were retained completely, which was confirmed by dynamic light scattering (DLS) and UV–vis spectroscopy of the permeate. In addition, we found that 25% of 25 nm PS beads passed through the membrane. Thus, the filtration cutoff of the membrane was between 25 and 39 nm. This is significantly smaller compared to the cutoff range found in diffusion experiments for the same membrane and might be the result of pressure driven flow compaction<sup>41</sup> that may occur either in the colloidal membrane or at the interface between the membrane and its support.

**“Neutral” Membranes.** Ultrafiltration in organic solvents has several applications,<sup>42</sup> but aqueous ultrafiltration is more widely used in various areas such as water purification,<sup>12</sup> protein separations and food industry.<sup>15</sup> Thus, we designed a reversibly formed membrane stable in water using the colloidal nanoparticles assembly. We discovered that nanoporous membranes can be prepared by the assembly of “hairy” silica spheres carrying poly(2-hydroxyethyl methacrylate), PHEMA, brushes (Figure 2A) from their ethanol solutions. The length of PHEMA brushes on 330 nm silica spheres required to form the free-standing porous membranes was  $\sim 15$  nm (determined by DLS) with the average molecular weight of  $\sim 6000$  g/mol (approximately 48 HEMA monomers per brush), as determined by thermogravimetric analysis (TGA) with the assumption of 0.5 HEMA chains per  $\text{nm}^2$ .<sup>37</sup> After ethanol evaporation, a solid material formed as smooth and evenly thick flat pieces of  $\sim 2$   $\text{cm}^2$  area. Their thickness could be controlled in the range from 0.4 to 0.7 mm by the concentration of the “hairy” spheres in colloidal solution in the 6–10 wt % range. There were significantly fewer cracks observed compared to the “acid–base” membranes. SEM images of the membranes (Figure 2B) showed closely packed yet disordered silica spheres. The SEM images of the membrane cross-section (Figure 2C) demonstrate that the “hairy” particles form a continuous assembly without mechanical defects and with a smooth surface.

We measured the flexural strength of the “neutral” membranes using the 4-point bending test, and found it to be  $0.5 \pm 0.1$  MPa. This flexural strength was significantly

smaller than that of sintered silica colloidal membranes ( $49 \pm 9$  MPa), which were prepared earlier.<sup>30</sup> This is expected as silica spheres in sintered membranes are connected to each other by strong Si–O–Si covalent bonds, while self-assembled “neutral” membranes form via noncovalent interactions between the PHEMA brushes. Despite the low flexural strength, the “neutral” membranes can be handled, sonicated, sandwiched between plastic or metal rings, and even dropped from 1 m height without breaking or cracking.

We found that “neutral” membranes were stable in water for at least 72 h, but softened in ethanol and acetonitrile within  $\sim 30$  min and completely dispersed in 24 h. Sonication accelerated this process and the membranes dispersed completely after 15 min of sonication. This behavior of “neutral” membranes likely arises from different solvation of PHEMA brushes in different solvents. PHEMA brushes swell significantly in organic solvents such as ethanol and methanol,<sup>43</sup> which causes the membranes to disassemble, whereas water solvates PHEMA to a smaller extent.<sup>43</sup>

According to the diffusion experiments in water, the cutoff of the “neutral” free-standing membranes made of 330 nm silica spheres was between 6 and 20 nm, as determined using G5 PAMAM dendrimer (6 nm in diameter), to which the membranes were permeable, and 20 nm gold nanoparticles, which were retained by the membrane. We believe that the much lower cutoff of the “neutral” membranes compared to the “acid–base” membranes comprising comparably sized silica spheres results from the swelling of PHEMA brushes in water, partially blocking the pores and reducing the effective pore size.<sup>26</sup>

Next, we prepared “neutral” membranes on regenerated cellulose support. The flux of water through the 1.3 mm thick membrane made of 460 nm PHEMA-modified silica spheres deposited regenerated cellulose support with on 0.2  $\mu\text{m}$  pores under 0.35 bar (5 psi) pressure was  $18 \text{ L m}^{-2} \text{ h}^{-1}$  (0.08 gpm). This flux is comparable to that of much thinner nanoporous polymeric ultrafiltration membranes with similar porosity.<sup>44</sup> As expected, applying a higher pressure resulted in a higher flux. The average water flux through the “neutral” membranes under 1.45 bar (21 psi) was  $103 \text{ L m}^{-2} \text{ h}^{-1}$  (0.45 gpm), which is

comparable or exceeds the flux of commercially available ultrafiltration membranes (such as 0.5 gpm for Watts hollow fiber ultrafiltration membrane with 0.2  $\mu\text{m}$  cutoff). Thus, “neutral” membranes can be potentially applied in ultrafiltration and water purification systems.

To demonstrate the tunability of the pore size in “neutral” membranes, we deposited silica spheres of two different diameters (280 and 460 nm) modified with PHEMA brushes from ethanol solution on top of nylon filters with 0.2  $\mu\text{m}$  pore size (Figure 3A–C). Supported “neutral” membranes could be

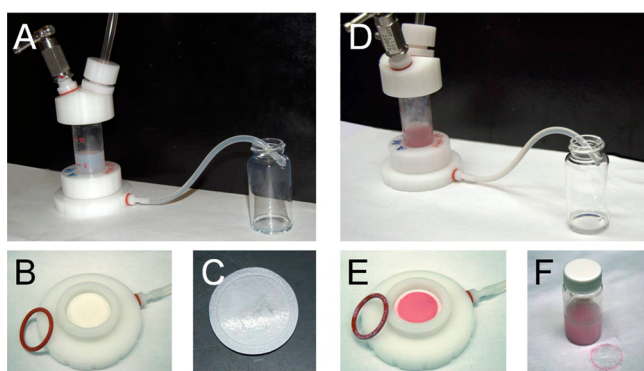


**Figure 3.** Preparation of supported “neutral” membrane and isolation of Au nanoparticles. (A) Formation of “neutral” membrane on cellulose support inside stirred cell. (B) Disassembled stirred cell with “neutral” membrane on support. (C) Supported membrane. (D) Ultrafiltration of 20 nm Au nanoparticles through “neutral” membrane made of 280 nm “hairy” silica spheres. (E) Disassembled stirred cell with Au nanoparticles trapped inside the “neutral” membrane. (F) Dispersed “neutral” membrane with Au nanoparticles in solution.

easily dispersed in ethanol and deposited again. We found that 6 nm dendrimer molecules passed through the membranes made of 280 nm “hairy” silica spheres, while 20 nm gold nanoparticles were completely retained (Figure 3D–F), which was confirmed by DLS and UV–vis spectroscopy of the permeate. The membrane made of PHEMA-modified 460 nm silica spheres possessed a larger cutoff: they were permeable to 20 nm gold nanoparticles, whereas 40 nm gold nanoparticles were completely retained. These cut-offs are smaller than those calculated for the close-packed silica colloidal crystals made of 280 and 460 nm spheres (44 and 70 nm, respectively), which we attribute to the swelling of PHEMA brushes in water. These results demonstrate that reversible “neutral” membranes are capable of size-selective ultrafiltration, and that their pore size can be easily tuned by changing the silica spheres size, and potentially polymer brush length.

The deposited “neutral” membrane with trapped gold nanoparticles could be dispersed in ethanol, forming a colloidal solution containing “hairy” silica spheres and gold nanoparticles. After the sonication, the heavier silica particles precipitate, which can be aided by centrifugation, whereas the small gold nanoparticles remain in solution and can be isolated. The collected silica spheres can be dispersed in ethanol and deposited to form the regenerated ultrafiltration membrane. To demonstrate the utility of this process, we separated a mixture of 20 and 40 nm Au nanoparticles using the “neutral” membrane made of 460 nm “hairy” silica spheres, as illustrated in Figure 4. After the formation of the colloidal membrane, the nanoparticle mixture was pushed through it under pressure, with 20 nm Au nanoparticles passing through the membrane

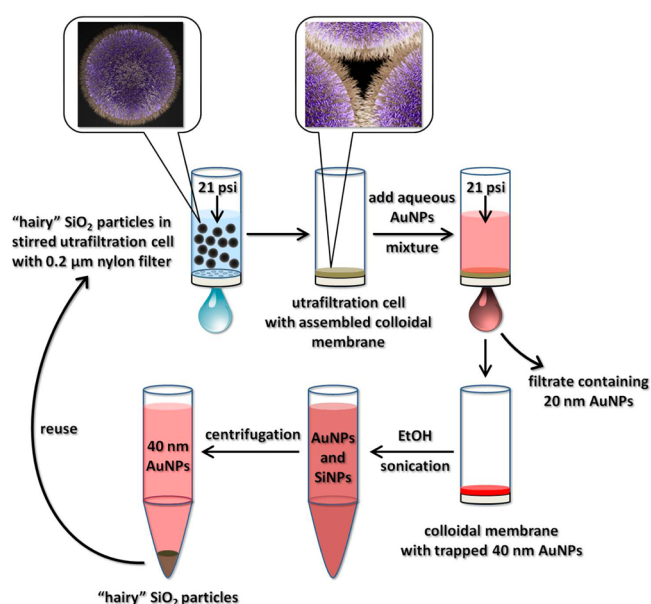


**Figure 4.** Schematic representation of the separation of 20 and 40 nm Au nanoparticles using the “neutral” ultrafiltration membrane and membrane recycling.

and 40 nm Au nanoparticles being retained. The latter were recovered by separating them from the “hairy” particles after the membrane was dispersed using ethanol. The “hairy” silica particles can be reassembled into membranes that function without the loss of separation performance.

## CONCLUSIONS

We developed a novel approach to the preparation of nanoporous membranes by reversible assembly of polymer brush-modified colloidal nanoparticles, which provides numerous advantages in terms of cleaning and reusing of the membrane without performance loss, as well as recovery of the retentate. The membranes are deposited from colloidal solutions and dispersed by switching the solvent. Membranes made of silica spheres modified with polymer brushes carrying acidic and basic functional groups are stable in organic solvents and disassemble in water, while membranes made of PHEMA-modified silica spheres are stable in water and disassemble in organic solvents. The membranes can withstand multiple cycles of assembly disassembly. Their filtration cutoff can be controlled by varying the silica sphere diameter and depends on the polymer brush structure. The membranes can be prepared as both free-standing materials and as supported films. The control over the pore size, high flux, durability, flexibility, time- and cost-efficiency, and the ability to recover the retentate and clean the membranes by disassembly makes them a promising material for ultrafiltration and size-selective separations. We are presently working on introducing active functional groups into the polymer brushes to prepare affinity membranes, as well as using polymer brushes that allow disassembly in response to stimuli other than solvent polarity. We are also studying the forces that lead to the formation of the colloidal membranes from the “hairy” particles.

## AUTHOR INFORMATION

### Corresponding Author

\*E-mail: i.zharov@utah.edu.

## Notes

The authors declare no competing financial interest.

## ACKNOWLEDGMENTS

This work was supported by the grants from the National Science Foundation (CHE-1213628 and DMR-1121252).

## REFERENCES

- (1) Cheryan, M. *Ultrafiltration and Microfiltration Handbook*; CRC Press: Boca Raton, FL, 1998; Chapter 1, pp 1–28.
- (2) Vandezande, P.; Gevers, L. E. M.; Vankelecom, I. F. J. Solvent Resistant Nanofiltration: Separating on a Molecular Level. *Chem. Soc. Rev.* **2008**, *37*, 365–405.
- (3) van Reis, R.; Zydney, A. Bioprocess Membrane Technology. *J. Membr. Sci.* **2007**, *297*, 16–50.
- (4) Deng, J.; Toh, C.-S. Impedimetric DNA Biosensor Based on a Nanoporous Alumina Membrane for the Detection of the Specific Oligonucleotide Sequence of Dengue Virus. *Sensors* **2013**, *13*, 7774–7785.
- (5) Hotta, K.; Yamaguchi, A.; Teramae, N. Deposition of Polyelectrolyte Multilayer Film on a Nanoporous Alumina Membrane for Stable Label-Free Optical Biosensing. *J. Phys. Chem. C* **2012**, *116*, 23533–23539.
- (6) Jeon, G.; Yang, S. Y.; Kim, J. K. Functional Nanoporous Membranes for Drug Delivery. *J. Mater. Chem.* **2012**, *22*, 14814–14834.
- (7) Wei, L.; Kawamoto, K. Upgrading of Simulated Syngas by Using a Nanoporous Silica Membrane Reactor. *Chem. Eng. Technol.* **2013**, *36*, 650–656.
- (8) Li, Q.; Cui, S.; Yan, X. Electrocatalytic Oxidation of Glucose on Nanoporous Gold Membranes. *J. Solid State Electrochem.* **2012**, *16*, 1099–1104.
- (9) Zhao, Q.; Yin, M.; Zhang, A.; Prescher, S.; Antonietti, M.; Yuan, J. Hierarchically Structured Nanoporous Poly(Ionic Liquid) Membranes: Facile Preparation and Application in Fiber-Optic pH Sensing. *J. Am. Chem. Soc.* **2013**, *135*, 5549–5552.
- (10) Adiga, S. P.; Jin, C.; Curtiss, L. A.; Monteiro-Riviere, N. A.; Narayan, R. J. Nanoporous Membranes for Medical and Biological Applications. *Wiley Interdiscip. Rev.: Nanomed. Nanobiotechnol.* **2009**, *1*, 568–581.
- (11) Stroeve, P.; Ileri, N. Biotechnical and Other Applications of Nanoporous Membranes. *Trends Biotechnol.* **2011**, *29*, 259–266.
- (12) Ulbricht, M. Advanced Functional Polymer Membranes. *Polymer* **2006**, *47*, 2217–2262.
- (13) Querelle, S. E.; Jackson, E. A.; Cussler, E. A.; Hillmyer, M. A. Ultrafiltration Membranes with a Thin Poly(Styrene) - B - Poly(Isoprene) Selective Layer. *ACS Appl. Mater. Interfaces* **2013**, *5*, 5044–5050.
- (14) Peinemann, K.-V.; Abetz, V.; Simon, P. F. W. Asymmetric Superstructure Formed in a Block Copolymer via Phase Separation. *Nat. Mater.* **2007**, *6*, 992–996.
- (15) Peng Lee, K.; Mattia, D. Monolithic Nanoporous Alumina Membranes for Ultrafiltration Applications: Characterization, Selectivity–Permeability Analysis and Fouling Studies. *J. Membr. Sci.* **2013**, *435*, 52–61.
- (16) Chang, Y.; Ling, Z.; Liu, Y.; Hu, X.; Li, Y. A Simple Method for Fabrication of Highly Ordered Porous  $\alpha$ -Alumina Ceramic Membranes. *J. Mater. Chem.* **2012**, *22*, 7445–7448.
- (17) Chiang, A. S. T.; Chao, K.-J. Membranes and Films of Zeolite and Zeolite-Like Materials. *J. Phys. Chem. Solids* **2001**, *62*, 1899–1910.
- (18) Krieg, E.; Weissman, H.; Shirman, E.; Shimoni, E.; Rybtchinski, B. A Recyclable Supramolecular Membrane for Size-Selective Separation of Nanoparticles. *Nat. Nanotechnol.* **2011**, *6*, 141–146.
- (19) Lu, Y.; Suzuki, T.; Zhang, W.; Moore, J. S.; Mariñas, B. J. Nanofiltration Membranes based on Rigid Star Amphiphiles. *Chem. Mater.* **2007**, *19*, 3194–3204.
- (20) Nunes, S. P.; Behzad, A. R.; Hooghan, B.; Sougrat, R.; Karunakaran, M.; Pradeep, N.; Vainio, U.; Peinemann, K.-V. Switchable pH-Responsive Polymeric Membranes Prepared via Block Copolymer Micelle Assembly. *ACS Nano* **2011**, *5*, 3516–3522.
- (21) Hilke, R.; Pradeep, N.; Madhavan, P.; Vainio, U.; Behzad, A. R.; Hooghan, B.; Sougrat, R.; Nunes, S. P.; Peinemann, K.-V. Block Copolymer Hollow Fiber Membranes with Catalytic Activity and pH-Response. *ACS Appl. Mater. Interfaces* **2013**, *5*, 7001–7006.
- (22) Altman, M.; Semiat, R.; Hasson, D. Removal of Organic Foulants from Feed Waters by Dynamic Membranes. *Desalination* **1999**, *125*, 65–75.
- (23) Ersahin, M. E.; Ozgun, H.; Dereli, R. K.; Ozturk, I.; Roest, K.; van Lier, J. B. A Review on Dynamic Membrane Filtration: Materials, Applications and Future Perspectives. *Bioresour. Technol.* **2012**, *122*, 196–206.
- (24) Park, M.-H.; Subramani, C.; Rana, S.; Rotello, V. M. Chemoselective Nanoporous Membranes via Chemically Directed Assembly of Nanoparticles and Dendrimers. *Adv. Mater.* **2012**, *24*, 5862–5866.
- (25) Mueggenburg, K. E.; Lin, X.-M.; Goldsmith, R. H.; Jaeger, H. M. Elastic Membranes of Close-Packed Nanoparticle Arrays. *Nat. Mater.* **2007**, *6*, 656–660.
- (26) He, J.; Lin, X.-M.; Chan, H.; Vukovic, L.; Kral, P.; Jaeger, H. M. Diffusion and Filtration Properties of Self-Assembled Gold Nanocrystal Membranes. *Nano Lett.* **2011**, *11*, 2430–2435.
- (27) Wang, L.; Xu, L.; Kuang, H.; Xu, C.; Kotov, N. A. Dynamic Nanoparticle Assemblies. *Acc. Chem. Res.* **2012**, *45*, 1916–1926.
- (28) Talpin, D. V.; Shevchenko, E. V.; Bodnarchuk, M. I.; Ye, X.; Chen, J.; Murray, C. B. Quasicrystalline Order in Self-Assembled Binary Nanoparticle Superlattices. *Nature* **2009**, *461*, 964–967.
- (29) Zharov, I.; Khabibullin, A. Surface-Modified Silica Colloidal Crystals: Nanoporous Materials with Controlled Molecular Transport. *Acc. Chem. Res.* **2014**, *47*, 440–449.
- (30) Bohaty, A. K.; Smith, J. J.; Zharov, I. Free-Standing Silica Colloidal Nanoporous Membranes. *Langmuir* **2009**, *25*, 3096–3101.
- (31) Ignacio-de Leon, P. A.; Zharov, I. Size-Selective Transport in Colloidal Nano-Frits. *Chem. Commun.* **2011**, *47*, 553–555.
- (32) Ignacio-de Leon, P. A.; Cichelli, J.; Abelow, A.; Zhukov, A.; Stoikov, I. I.; Zharov, I. Silica Colloidal Membranes with Enantioselective Permeability. *Isr. J. Chem.* **2014**, *54*, 767–773.
- (33) Stöber, W.; Fink, A.; Bohn, E. Controlled Growth of Monodisperse Silica Spheres in the Micron Size Range. *J. Colloid Interface Sci.* **1968**, *26*, 62–69.
- (34) Schepelina, O.; Poth, N.; Zharov, I. pH-Responsive Nanoporous Silica Colloidal Membranes. *Adv. Funct. Mater.* **2010**, *20*, 1962–1969.
- (35) Smith, J. J.; Zharov, I. Preparation and Proton Conductivity of Sulfonated Polymer-Modified Sintered and Self-Assembled Silica Colloidal Crystals. *Chem. Mater.* **2009**, *21*, 2013–2019.
- (36) Khabibullin, A.; Zharov, I. Nanoporous Membranes with Tunable Pore Size by Pressing/Sintering Silica Colloidal Spheres. *ACS Appl. Mater. Interfaces* **2014**, *6*, 7712–7718.
- (37) Choi, J.; Dong, H.; Matyjaszewski, K.; Bockstaller, M. R. Flexible Particle Array Structures by Controlling Polymer Graft Architecture. *J. Am. Chem. Soc.* **2010**, *132*, 12537–12539.
- (38) Choi, J.; Hui, C. M.; Pietrasik, J.; Dong, H.; Matyjaszewski, K.; Bockstaller, M. R. Toughening Fragile Matter: Mechanical Properties of Particle Solids Assembled from Polymer-Grafted Hybrid Particles Synthesized by ATRP. *Soft Matter* **2012**, *8*, 4072–4082.
- (39) Singh, K.; Tirumkudulu, M. Cracking in Drying Colloidal Films. *Phys. Rev.* **2007**, *98* (218302), 1–4.
- (40) Malavolta, L.; Oliveira, E.; Cilli, E. M.; Nakaie, C. R. Solvation of Polymers as Model for Solvent Effect Investigation: Proposition of a Novel Polarity Scale. *Tetrahedron* **2002**, *58*, 4383–4394.
- (41) Connolly, J. A. D.; Podladchikov, Y. Y. Compaction-Driven Fluid Flow in Viscoelastic Rock. *Geodinamica Acta* **1998**, *11*, 55–84.
- (42) Cai, W.; Sun, Y.; Piao, X.; Li, J.; Zhu, S. Solvent Recovery from Soybean Oil/Hexane Miscella by PDMS Composite Membrane. *Chin. J. Chem. Eng.* **2011**, *19*, 575–580.
- (43) Campan, R.; Cazaux, F.; Coqueret, X. Controlled Swelling of Poly(Hydroxyethyl Methacrylate) Hydrogels by Photochemical



Grafting of Hydrophobic Acrylates. *Macromol. Mater. Eng.* **2002**, *287*, 924–930.

(44) Yang, S. Y.; Ryu, I.; Kim, H. Y.; Kim, J. K.; Jang, S. K.; Russell, T. P. Nanoporous Membranes with Ultrahigh Selectivity and Flux for the Filtration of Viruses. *Adv. Mater.* **2006**, *18*, 709–712.